PHYSICAL REVIEW A **80**, 051802(R) (2009)

Attraction and repulsion of parallel femtosecond filaments in air

Hua Cai, Jian Wu,* Peifen Lu, Xueshi Bai, Liang'en Ding, and Heping Zeng†
State Key Laboratory of Precision Spectroscopy, East China Normal University, Shanghai 200062, China
(Received 8 June 2009; published 16 November 2009)

We present an approach to explore and control nonlinear interactions between two orthogonally polarized femtosecond filaments launched parallel in air. The self-phase and cross-phase modulations due to the Kerr effect and cross-(de)focusing induced by the plasma and molecular alignment were distinctly identified resulting in attraction and repulsion of parallel filaments with different spatiotemporal proximities. Their interaction ranges were analyzed by comparing the interaction-induced displacements of parallel filaments at different initial separations. As proved by field-free displacements of parallel filaments around the impulsive rotational Raman excitation of the diatomic molecules in air, the molecular alignment exhibited a relatively longer interaction range than that of the plasma defocusing and the Kerr effect.

DOI: 10.1103/PhysRevA.80.051802 PACS number(s): 42.65.Sf, 42.50.Md, 42.65.Re, 52.38.Hb

Nonlinear interactions of self-guided wave-packets (filaments) show fascinating particlelike features [1], such as light-bullet fusion, fission, and spiraling [2–8], which might stimulate vast applications by using nonlinearly coupled multiple filaments instead of single ones. Traditionally, interactions of light bullets occur in the region of close spatiotemporal proximity. The incoherent couplings between far-delayed or spatially separated intense ultrashort pulses have been so far unexplored. Various mechanisms, such as Kerr and higher-order nonlinear optical responses, molecular rotational Raman response, and ionization-induced plasma, act together to guide or modulate nonlinear interactions of intense light bullets. Filaments experience complicated nonlinear couplings in the spatiotemporally overlapped region due to the interplays and competitions of these different nonlinear effects. This makes the intrinsic physics and origins of filament interaction difficult to understand. Therefore, a straightforward approach is needed to distinguish different physical mechanisms governing the spatiotemporal light bullet interaction. This would stimulate experimental breakthroughs not only in exploring their nonlinear interactions but also in establishing a robust and field-free technique to control filament interaction for promising atmospheric applications. In particular, it may serve as the basis to manipulate many important and useful nonlinear optical processes in strongly coupled filaments [9–15], such as secondary radiation emission in the terahertz region, nonlinear frequency conversion, and wavelength-tunable few-cycle pulse generation.

In this Rapid Communication, we demonstrate a straightforward method to distinguish filament interactions originating from the Kerr effect, plasma defocusing, and molecular alignment. Spatiotemporally overlapped intense femotosecond (fs) filaments typically interact via the Kerr effect and ionization-induced plasma, which lead the local refractive index to increase and decrease in filaments, respectively. For a molecular gas, the molecular alignment [16–19] affect the filaments coupling due to the orientation-dependent modulation of the local refractive index with prealigned molecules [20–22] and alter the plasma density due to the dependence of ionization cross sections on the relative molecular orientation to the field polarization [23]. Intense fs filaments in air are thus coupled by the local changes in the refractive index induced by the Kerr nonlinearity, plasma, and molecular alignment. Their interactions were analyzed straightforwardly by comparing the displacements of parallel filaments launched at various pump-probe delays with different initial separations. Molecular alignment induce a relatively longer interaction range than the Kerr effect and plasma defocusing. Field-free controllable filament interaction could be further realized around the periodic revivals of the pre-excited rotational wave packets in air.

As schematically illustrated in Fig. 1, the fs pulses (35 fs, 800 nm, and 1 kHz) were firstly split into *s*-polarized pump and *p*-polarized probe pulses, which were slightly focused with two properly positioned lenses ($f=1$ m) in their corresponding arms. They were recombined with a thin film polarizer to get two parallel filaments in air with initial spatial separations of several ten to hundred μm. The positive delays account for the pump pulse ahead of the probe one, and the zero delay was ascertained by accurately measuring the maximum second harmonic generation with a frequency-doubling crystal. The pump and probe pulse energies were measured to be ~1.57 and 0.76 mJ before filamentation, respectively. In order to investigate the interaction dynamics of these parallel launched filaments, the ionization-induced

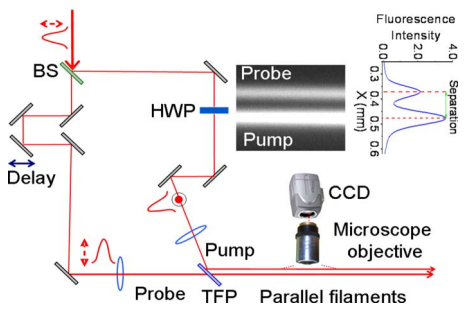

FIG. 1. (Color online) Schematic illustration of the experimental setup. The insert shows the measured fluorescence images and profiles of pump and probe filaments.

*jwu@phy.ecnu.edu.cn
†hpzeng@phy.ecnu.edu.cn

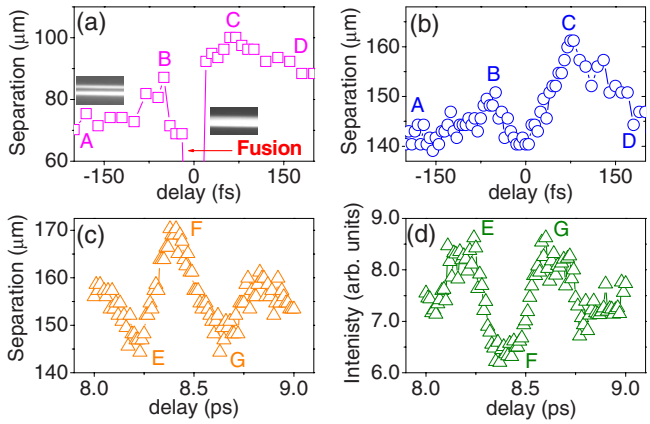

FIG. 2. (Color online) The separations between pump and probe filaments versus the time delay with initial separations of (a) 70 and (b) 140 μm, respectively. The inset of (a) show the measured fluorescence images of pump and probe filaments near −200 fs and at zero delay. The measured (c) separation between the pump and probe filaments and (d) the fluorescence intensity of the probe filament versus the time delay.

fluorescence [24] of the pump and probe filaments were collected by a microscope objective (10×) and detected by a monochrome digital charge coupled device (CCD). The typical fluorescence images and profiles of the parallel filaments are shown in the inset of Fig. 1.

We first studied the attraction and repulsion of two parallel filaments near zero delay (−200–200 fs). The observed filament displacements are shown in Figs. 2(a) and 2(b). With the pump filament delayed by 100–200 fs behind the probe one (around delay-A), the parallel filaments were separated by almost the same distances of the initially launched ones (70 or 140 μm), indicating no filament interactions within this range of delay. However, as the pump filament propagated ahead of the probe one by 100–200 fs (around delay-D), the parallel filaments were repulsed up to 90 and 145 μm, respectively. A larger displacement around delay-D than that around delay-A proved that the probe filament was influenced more significantly by the pump one. Moreover, the pump filament kicked the probe one to a larger displacement for a smaller initial spatial separation [Figs. 2(a)]. All these arose from the difference in pump and probe pulse intensities. As the strong pump pulse ahead produced a larger plasma density than the relatively weak probe pulse ahead, a larger reduction in the refractive index was induced in the pump filament channel, which consequently resulted in a larger plasma-induced repulsion of the parallel filaments.

Kerr-induced filament interaction was mainly due to cross-phase modulation (XPM) between parallel filaments of partially spatiotemporal overlapping. This could be clearly observed by varying the delay between the pump and probe pulses within the pulse duration (−35–35 fs). For the initial filament separation of ~70 μm, as shown in Fig. 2(a), the pump and probe filaments were attracted to each other and eventually fused together near the zero delay. For the initial filament separation of ~140 μm, the Kerr-induced filament attraction became weaker and no filament fusions were observed near zero delay, as shown in Fig. 2(b). The separation between the pump and probe filaments at zero delay [Fig. 2(b)] was almost the same as the initial separation, indicating a counterbalance between the plasma-induced repulsion and Kerr-induced attraction of the synchronized parallel filaments. This confirmed a complex interaction between the plasma cross-defocusing and Kerr-induced filament attraction.

When the probe or pump pulses propagated around 80 fs ahead, as denoted by delay-B and delay-C in Figs. 2(a) and 2(b), parallel filaments initially separated by 70 or 140 μm were repulsed up to spatial separations of 90 and 100 μm or 150 and 160 μm, respectively. Note that the parallel filaments had negligible temporal overlappings at delay-B and delay-C, the Kerr nonlinear couplings played a negligible role in filament interaction. The enhanced repulsion should come from the local refractive index modulation induced by the molecular alignment, which showed a slight delayed response to the excitation pulse. There was also a remarkable difference in filament displacements between delay-B (probe ahead) and delay-C (pump ahead) manifested by the fact that the filament displacements at delay-B were smaller than those at delay-C. The strong pump pulse propagating ahead produced more significant influence on the filament repulsion with an enhanced degree of molecular alignment than the probe pulse ahead. For the initial separation of ~140 μm, where plasma induced cross-defocusing became weaker filament repulsions were still observed at both delay-B and delay-C, suggesting that molecular alignment could induce filament interaction in a longer range compared to plasma defocusing.

Impulsive molecular alignment [16–19] was achieved through rotational Raman excitation by intense ultrashort laser pulses. Figure 3(a) shows the experimentally measured weak field polarization signal $\sim(\langle\langle\cos^2\theta_{\parallel}\rangle\rangle-1/3)^2$, where $\theta_{\parallel}$ is the angle between the molecular axis and pump polarization. In the experimental measurements, we rotated the polarization of the pre-attenuated probe pulse by 45° with respect to the pump polarization. The pump and probe pulses were noncollinearly crossed at an angle of ~2°. The field component with polarization perpendicular to the incident probe polarization was selected by an α-BBO polarizer and analyzed by a lock-in amplifier (SR830, Stanford) at various pump-probe delays. Since the polarizations of pump and probe pulses were orthogonal to each other, we calculated the molecular alignment revival $\langle\langle\cos^2\theta_{\perp}\rangle\rangle=(1-\langle\langle\cos^2\theta_{\parallel}\rangle\rangle)/2$, where $\theta_{\perp}$ is the angle between the molecular axis and the field polarization of the probe pulse. The space- and time-dependent refractive index modulation due to molecular alignment reads as $\delta n_{mol\perp}(r,t)=2\pi(\rho_0\Delta\alpha/n_0)[\langle\langle\cos^2\theta_{\perp}\rangle\rangle(r,t)-1/3]+\delta n_{rR\perp}(r,t)$ [20], which increases and decreases for parallel $(\langle\langle\cos^2\theta_{\perp}\rangle\rangle>1/3)$ and perpendicular $(\langle\langle\cos^2\theta_{\perp}\rangle\rangle<1/3)$ orientated molecules, respectively. As shown in Fig. 3(b), the rotational Raman response was delayed about ~80 fs with respect to the excitation pulse envelope, which was consistent with the experimental observation of filament repulsions at delay-B and delay-C in Figs. 2(a) and 2(b). As we measured experimentally, about 20% of the incident energy was contained in the pump filament with a radius of ~70 μm and a pulse duration of ~60 fs, while the probe filament

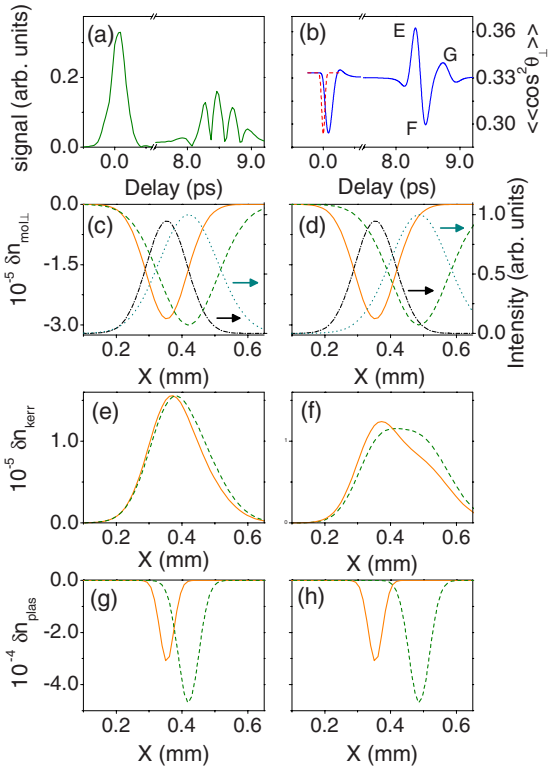

FIG. 3. (Color online) (a) The measured molecular alignment signal of air proportional to $(\langle\langle\cos^2\theta_{\parallel}\rangle\rangle-1/3)^2$ and (b) the calculated $\langle\langle\cos^2\theta_{\perp}\rangle\rangle$ versus the time delay. The calculated profiles of [(c) and (d)] $\delta n_{mol\perp}$, [(e) and (f)] δn_{Kerr}, and [(g) and (h)] δn_{plas} when the parallel pump (olive-dash) and probe (orange-solid) filaments are launched with separations of 70 (left) and 140 μm (right), respectively. The dash-dotted and dotted lines in (c) and (d) represent the intensity profiles of the pump and probe filaments deduced from the measured fluorescence profiles.

contained about 30% of the incident energy with a radius of ~50 μm and a pulse duration of ~90 fs. The peak intensities of the pump and probe pulses were accordingly estimated to be $I_{pump}\sim 3.4\times 10^{13}$ and $I_{probe}\sim 3.2\times 10^{13}$ W/cm^2, which consist with the peak intensity clamping inside the filament core [25]. Figure 3(c)(dotted and dash-dotted curves) shows the intensity profiles of the pump and probe filaments $I(r)$, which were derived according to $N_e(r)=N_{air}[0.21\sigma_{O_2}I(r)^8\tau+0.78\sigma_{N_2}I(r)^{11}\tau]$ [24], where the electron density $N_e(r)$ is proportional to the fluorescence intensity profiles as measured in our experiments, N_{air} denotes the number density of air, τ is the pulse duration, and $\sigma_{O_2}=2.81\times 10^{-96}$ s^{-1} cm^{16}/W^8, $\sigma_{N_2}=6.31\times 10^{-140}$ s^{-1} cm^{22}/W^{11} are the ionization cross sections of O_2 and N_2, respectively. Figure 3(c) also shows the calculated $\delta n_{mol\perp}$ from the molecular alignment excited by the pump and probe pulses. The pump pulse induced a larger $\delta n_{mol\perp}$ around the probe peak than that produced by probe pulse at the pump peak, giving rise to an obvious filament repulsion at delay-C, as observed in Figs. 2(a) and 2(b). For an enlarged initial separation of ~140 μm, as shown in Fig. 3(d), $\delta n_{mol\perp}$ from the molecular alignment excited by the pump and probe pulses were decreased at the probe and pump peaks, respectively, it was still sufficient to produce noticeable filament repulsions as observed in Fig. 2(b).

The most significant nonlinear couplings between spatiotemporally overlapped filaments came from the Kerr nonlinearity with the locally increased refractive index [26]. On the basis of the spatial profiles of the pump and probe filaments, we calculated the refractive index modulations of $\delta n_{Kerr}(r,t)\sim n_2 I_{pump}+n_2^{XPM}I_{probe}$ and $\delta n_{Kerr}(r,t)\sim n_2 I_{probe}+n_2^{XPM}I_{pump}$, respectively, in the pump and probe filaments, where $n_2=3.2\times 10^{-19}$ cm^2/W is the Kerr nonlinear coefficient of air and accounts for the self-phase modulation and $n_2^{XPM}=2n_2/3$ represents the Kerr effect induced by the XPM of the orthogonally polarized pump (or probe) pulse [26,27]. As shown in Fig. 3(e), δn_{Kerr} in the pump and probe filaments exhibited almost overlapped profiles and accordingly, filament fusion was facilitated as observed in Fig. 2(a). For a large initial filament separation, δn_{Kerr} in the pump and probe filaments [Fig. 3(f)] were accurately separated with decreased peak values, where no filament fusions were observed as in Fig. 2(b).

Molecular ionization in filaments affected the parallel filaments due to the plasma-induced local reduction of the refractive index as $\delta n_{plas}\sim -\rho(r,t)/(2\rho_c)$ [25], where ρ is the electron density and ρ_c (~1.7×10^{21} cm^{-3} at 800 nm) is the critical plasma density. We considered both the ionization of O_2 and N_2 in air as discussed above, and the electron densities in the pump and probe filaments were estimated to be ~1.6×10^{18} and 1.0×10^{18} cm^{-3}, respectively. The plasma-induced modulation of the refractive index δn_{plas} by the pump and probe pulses are plotted in Fig. 3(g) with the initial filament separation of ~70 μm. The absolute value of δn_{plas} produced by the pump ionization was much larger than that by the probe. Therefore, the influence of the probe ionization was relatively small, which was demonstrated in the experiment by the larger filament displacement around delay-D than that around delay-A [see Figs. 2(a) and 2(b)]. When the initial separation of filaments was changed to ~140 μm, δn_{plas} induced by the pump and probe filaments were spatially separated as shown in Fig. 3(h), leading to nearly vanished plasma influence as observed in Fig. 2(b).

The long interaction range of the molecular alignment was further demonstrated for an even larger initial filament separation (~159 μm). The delay between pump and probe filaments was turned to 8.0–9.0 ps, which contained the full-revival of molecular N_2 and the three-quarter revival of molecular O_2. As shown in Fig. 3(b), the orientation of molecules was parallel to the probe polarization at delay-E and delay-G, while it was perpendicular to the probe polarization at delay-F. Therefore, the probe filament was attracted by the pump filament at delay-E and delay-G for $\delta n_{mol\perp}>0$ and repulsed at delay-F for $\delta n_{mol\perp}<0$, as observed in Fig. 2(c). A modulation of the fluorescence intensity of probe pulse was observed. As shown in Fig. 2(d), this modulation followed the molecular alignment revivals. It could be well understood by the fact that diatomic molecules parallel aligned to the filed polarization are much more easily ionized than those perpendicularly aligned [23].

In summary, we observed strong interactions between two parallel filaments around zero time delay and field-free molecular alignment revivals. The molecular alignment was

demonstrated to have a relatively longer interaction range than the Kerr and plasma effects, which further occurred periodically around the field-free revivals, providing a promising approach to remotely control filament interaction.

This work was supported by National Natural Science Fund (Grants No. 10990101, No. 10525416, and No. 10804032) and National Key Project for Basic Research (Grant No. 2006CB806005).

[1] D. J. Mitchell, A. W. Snyder, and L. Poladian, Phys. Rev. Lett. **77**, 271 (1996).
[2] G. I. Stegeman and M. Segev, Science **286**, 1518 (1999).
[3] C. Rotschild *et al.*, Nat. Phys. **2**, 769 (2006).
[4] M.-F. Shih, M. Segev, and G. Salamo, Phys. Rev. Lett. **78**, 2551 (1997).
[5] S. Tzortzakis *et al.*, Phys. Rev. Lett. **86**, 5470 (2001).
[6] A. W. Snyder and A. P. Sheppard, Opt. Lett. **18**, 482 (1993).
[7] T. T. Xi, X. Lu, and J. Zhang, Phys. Rev. Lett. **96**, 025003 (2006).
[8] B. Shim, S. E. Schrauth, C. J. Hensley, P. Hui, A. D. Slepkov, A. A. Ishaaya, L. T. Vuong, and A. L. Gaeta, in *Frontiers in Optics*, OSA Technical Digest (Optical Society of America, 2008), paper FTuV4.
[9] Y. Liu *et al.*, Phys. Rev. Lett. **99**, 135002 (2007).
[10] J. Dai, X. Xie, and X. C. Zhang, Phys. Rev. Lett. **97**, 103903 (2006).
[11] A. Houard, Y. Liu, B. Prade, V. T. Tikhonchuk, and A. Mysyrowicz, Phys. Rev. Lett. **100**, 255006 (2008).
[12] J. Yu *et al.*, Opt. Lett. **26**, 533 (2001).
[13] R. A. Bartels *et al.*, Opt. Lett. **28**, 346 (2003).
[14] K. Hartinger and R. A. Bartels, Opt. Lett. **33**, 1162 (2008).
[15] J. Wu, H. Cai, A. Couairon, and H. Zeng, Phys. Rev. A **79**, 063812 (2009).
[16] H. Stapelfeldt and T. Seideman, Rev. Mod. Phys. **75**, 543 (2003).
[17] A. Hishikawa, A. Iwamae, and K. Yamanouchi, Phys. Rev. Lett. **83**, 1127 (1999).
[18] V. Renard *et al.*, Phys. Rev. Lett. **90**, 153601 (2003).
[19] M. D. Poulsen, T. Ejdrup, H. Stapelfeldt, E. Hamilton, and T. Seideman, Phys. Rev. A **73**, 033405 (2006).
[20] J. Wu *et al.*, Opt. Lett. **33**, 2593 (2008).
[21] S. Varma, Y. H. Chen, and H. M. Milchberg, Phys. Rev. Lett. **101**, 205001 (2008).
[22] J. Wu *et al.*, Opt. Lett. **34**, 3211 (2009).
[23] I. V. Litvinyuk *et al.*, Phys. Rev. Lett. **90**, 233003 (2003).
[24] J. Bernhardt *et al.*, Appl. Phys. B: Lasers Opt. **91**, 45 (2008).
[25] A. Couairon and A. Mysyrowicz, Phys. Rep. **441**, 47 (2007).
[26] G. P. Agrawal, *Nonlinear Fiber Optics* (Academic Press, San Diego, 2001).
[27] P. Béjot *et al.*, Opt. Express **16**, 7564 (2008).